Electrostatically Directed Visual Fluorescence Response of DNA-Functionalized Monolithic Hydrogels for Highly Sensitive Hg^{2+} Detection

*Kevin A. Joseph, Neeshma Dave and Juewen Liu**

Department of Chemistry, Waterloo Institute for Nanotechnology, University of Waterloo,

200 University Avenue West, Waterloo, Ontario, N2L 3G1, Canada Email:

liujw@uwaterloo.ca

Received: November 4, 2010

Accepted: January 31, 2011

Published: February 16, 2011

ABSTRACT

Hydrogels are crosslinked hydrophilic polymer networks with low optical background and high loading capacity for immobilization of biomolecules. Importantly, the property of hydrogel can be precisely controlled by changing the monomer composition. This feature, however, has not been investigated in the rational design of hydrogel-based optical sensors. We herein explore electrostatic interactions between an immobilized mercury binding DNA, a DNA staining dye (SYBR Green I), and the hydrogel backbone. A thymine-rich DNA was covalently functionalized within monolithic hydrogels containing a positive, neutral, or negative backbone. These hydrogels can be used as sensors for mercury detection since the DNA can selectively bind Hg^{2+} between thymine bases inducing a hairpin structure. SYBR Green I can

then bind to the hairpin to emit green fluorescence. For the neutral or negatively charged gels, addition of the dye in the absence of Hg^{2+} resulted in intense yellow background fluorescence, which was attributed to SYBR Green I binding to the unfolded DNA. We found that by introducing 20% positively charged allylamine monomer, the background fluorescence was significantly reduced. This was attributed to the repulsion between positively charged SYBR Green I by the gel matrix as well as the strong binding between the DNA and the gel backbone. The signal-to-background ratio and detection limit was respectively improved by six and nine-fold using the cationic gel instead of neutral polyacrylamide gel. This study helps understand the electrostatic interaction within hydrogels, showing that hydrogels can not only serve as a high capacity matrix for sensor immobilization, but can also actively influence the interaction between involved molecules.

Keywords: hydrogels, electrostatic interactions, charge, mercury, DNA, fluorescence

INTRODUCTION

Hydrogels are crosslinked hydrophilic polymers and they have been functionalized with many biomolecules, including DNA, to make stimuli-responsive materials and sensors (1-18). Most of these sensors, however, rely on hydrogel phase transition or volume change for detection. We are interested in developing hydrogel-based optical sensors with a visual fluorescent or colorimetric output to omit the need for analytical instrument. Hydrogels are ideal for optical sensor immobilization because of their good biocompatibility, large sensor loading capacity, and very low optical background. In addition, hydrogel backbone property such as charge and hydrophobicity can be preciously tuned by mixing different monomers, allowing further control of sensor performance. Although the effect of electrostatic interactions within hydrogels has been reported in the literature (19-22), no one has yet demonstrated the rational design of hydrogel-based optical sensors by tuning gel backbone charge. Such studies are important because electrostatic interactions may serve as a filter to selectively exclude interfering molecules and improve sensor performance. At the same time, we can gain fundamental understandings on the interaction between polyelectrolyte hydrogels and charged molecules through the sensor response.

We recently immobilized a mercury binding DNA within a polyacrylamide hydrogel (17). This DNA is rich in thymine and Hg^{2+} can be selectively chelated by thymines to fold the DNA into a hairpin (23). The unfolded anionic DNA can bind positively charged SYBR Green I (SG) to give strong yellow background fluorescence in the absence of Hg^{2+}; while in the presence of Hg^{2+}, a green fluorescence is observed. With the convenient optical readout, this system can serve as a model to understand electrostatic interactions within hydrogels. Polyacrylamide is a neutral hydrogel and it does not have much effect on DNA in terms of electrostatic interactions. In this work, we demonstrate that by adding a cationic allylamine monomer, the interaction between SG and DNA in the absence of Hg^{2+} is disrupted, giving very low background fluorescence. Since hydrogels are highly porous, we also found that the electrostatic force needs to reach a long range to be effective. In an aqueous solution, this means a long Debye length and a low ionic strength. With these fundamental understandings, we were able to improve the signal-to-background ratio by 6-fold and a detection limit of 1.1 nM was achieved, representing a 9-fold improvement over the neutral gel. Compared to many other fluorescent (24-31), colorimetric (32-41), and electrochemical (42-45) sensors based on the same mercury recognition mechanism, the detection limit of our cationic hydrogel is among the highest.

MATERIALS AND METHODS

Chemicals. The acrydite-modified mercury binding DNA, its complementary DNA, and the cytidine rich control DNA (acrydite-5′-CCCCCCCCCCCCCCCCGCCCGCC) were purchased from Integrated DNA Technologies (Coralville, IA) and were purified by standard desalting. Acrylamide/bis-acrylamide 29:1 40% gel stock solution, bromophenol blue, ammonium persulphate (APS), and N,N,N',N'tetramethylethylenediamine (TEMED) were purchased from VWR (Mississauga, Ontario, Canada). Allylamine, 2-acrylamido-2-methyl-1-propanesulfonic acid (AMPS), bis-acrylamide, mercury perchloride, copper sulfate, zinc chloride, manganese chloride, cobalt chloride, lead acetate, magnesium chloride, cadmium chloride, lithium chloride, barium chloride, and calcium chloride were obtained from Sigma-Aldrich. Sodium nitrate, sodium hydroxide, and tris(hydroxymethyl)aminomethane (Tris) were

purchased from Mandel Scientific (Guelph, Ontario, Canada). 10,000□ SYBR Green I (SG) in dimethyl sulfoxide (DMSO) was purchased from Invitrogen (Carlsbad, CA).

Synthesis of DNA-functionalized hydrogels. First the monomer stock solutions were prepared. AMPS was made to be 50% (w/v) and allylamine was diluted to 35% (v/v). These solutions were adjusted to pH 8.0 using NaOH and HNO_3. The initiator solution was prepared daily by dissolving 50 mg APS and 25 μL TEMED in 500 μL H_2O. To prepare a neutral 6% hydrogel, 2 M $NaNO_3$ (20 μL), 0.5 M pH 8.0 Tris nitrate (40 μL), acrylamide/bis-acrylamide 29:1 40% solution (60 μL), 500 μM DNA (6 μL), and lastly the initiator solution (20 μL) were added to 254 μL H_2O. The gels were made to be 70 μL each in a 96 well plate and were allowed to polymerize for 1 hr. To prepare a 6% positively-charged hydrogel containing allylamine/acrylamide, 2 M $NaNO_3$ (10 μL), 0.5 M pH 8 Tris nitrate (20 μL), acrylamide/bis-acrylamide 29:1 40% solution (30 μL), 35% allylamine (34 μL), 2.5% bis-acrylamide (17 μL), 500 μM DNA (6 μL), and lastly the initiator solution (10 μL) were added to 73 μL H_2O. The gels were prepared to be 33 μL each in a 96 well plate. After swelling in buffer A (20 mM $NaNO_3$, 8 mM Tris nitrate, pH 8.0), the final volume of the gel was ~70 μL. To prepare a 5.5% negatively-charged hydrogel, 2 M $NaNO_3$ (5 μL), 0.5 M pH 8 Tris nitrate (10 μL), acrylamide/bis-acrylamide 29:1 40% solution (37 μL), 50% AMPS (24 μL), 2.5% bis-acrylamide (11.5 μL), 500 μM DNA (7.5 μL), and lastly the initiator solution (5 μL) were mixed. The gels were made to be 20 μL each on a sheet of parafilm. Gels with other formulations were prepared in a similar way but with different monomer concentrations. The goal was that after swelling in buffer A, the gels all contained roughly the same DNA concentration and have a similar gel percentage.

Swelling experiment. To study the swelling of the gels in water and in buffer, the gels (6% and 70 μL each before swelling) were first soaked overnight in H_2O, followed by soaking in 5 μM bromophenol blue dye for 1 hr. Lastly, the gels were soaked in H_2O or buffer A for 1 hr and weighed to measure the mass

after wash. The swelling ratio was calculated by dividing the final mass by the mass of the monomers. The gels were also imaged by a digital camera (Canon PowerShot SD1200 IS).

Mercury detection. To detect Hg^{2+}, the gels were soaked in 50 mL water twice (first for five hours and then overnight) to completely remove free monomers, non-incorporated DNA, and initiators. To optimize the detection condition, the gels were individually placed in 1.5 mL microcentrifuge tubes containing 1 mL buffer A. After that, 2 μM Hg^{2+} and 3 μL 500 μM SG were added. The gels were soaked at room temperature and at designated time points they were excited using a hand-held UV lamp at 365 nm and imaged with the digital camera. Alternatively the fluorescence intensity was quantified using a gel documentation system (Alpha Innotech FluorChem FC2) at 365 nm excitation and with the SYBR Green filter. To measure the sensitivity of the sensors, the gels were soaked in 50 mL of varying concentrations of Hg^{2+} in the presence of 2 mM Tris nitrate, pH 8.0. After soaking overnight to allow mercury binding, the gels were transferred to 1.5 mL microcentrifuge tubes, each containing 1 mL of buffer A and 3 μL of 500 μM SG. After 1 hr, the gels were imaged. Lake Ontario water samples were collected from Colonel Samuel Smith Park in Toronto, Ontario, Canada. Since ICP-MS analysis showed no detectable mercury, $Hg(ClO_4)_2$ was added to simulate contaminated water (no additional salt or buffer was added). Each sensor (gels containing 20% allylamine) was soaked in 50 mL of such spiked water sample overnight and was subsequently transferred into 1.5 mL microcentrifuge tubes containing 1 mL buffer A. 3 μL of 500 □M SG was added. After 1 hr, these gels were imaged.

RESULTS AND DISCUSSION

DNA immobilization and signal generation. Mercury is a highly toxic heavy metal and is known to cause serious health problems including brain and kidney damage and immune system dysfunction (24, 46, 47). Therefore, detection of mercury in water has attracted a lot of research interests (24). We recently immobilized a mercury binding DNA in a monolithic polyacrylamide hydrogel (17). The sequence (see Figure 1A) was slightly modified from that reported by Liu and co-workers (28). Each DNA contained

seven Hg^{2+} binding sites. To generate a fluorescence signal, SYBR Green I (SG) was also included in the sensor system. In the absence of Hg^{2+}, if the DNA and SG concentrations were low (e.g. 15 and 90 nM, respectively), SG was almost non-fluorescent because the dye had a low affinity for unfolded single-stranded (ss)-DNA. In the presence of Hg^{2+}, the DNA folded into a hairpin and SG could bind to the double-stranded (ds) region to give a large fluorescence enhancement (e.g. >9-fold) (17, 28). To visually observe the fluorescence signal, however, higher DNA and SG concentrations were required, which also led to increased background signal. For example, with 1 μM DNA and 6 μM SG, addition of Hg^{2+} increased the fluorescence intensity by only ~1.5-fold (Figure 2A). At the same time, the emission peak blue shifted from 526 nm (yellow fluorescence) to 521 nm (green fluorescence). With an even higher DNA concentration in gel (e.g. ~5 μM), only ~30% fluorescence increase was observed (17). These experiments confirm that SG has a much lower binding affinity for ss-DNA compared to ds-DNA. In our system, SG can bind low nanomolar ds-DNA but ss-DNA has to reach micromolar to bind.

For covalent immobilization, the 5′-end of the DNA was modified with an acrydite so that the DNA can co-polymerize in the gel matrix. Acrylamide is not charged around neutral pH (Figure 1B). To study the effect of hydrogel backbone charge, two new monomers were tested and bis-acrylamide was used as a crosslinker to prepare all the gels. The cationic monomer was allylamine (Figure 1C), and the anionic monomer was 2-acrylamido-2-methyl-1-propanesulfonate (AMPS, Figure 1D). The structure of positively charged SG is shown in Figure 1E (48).

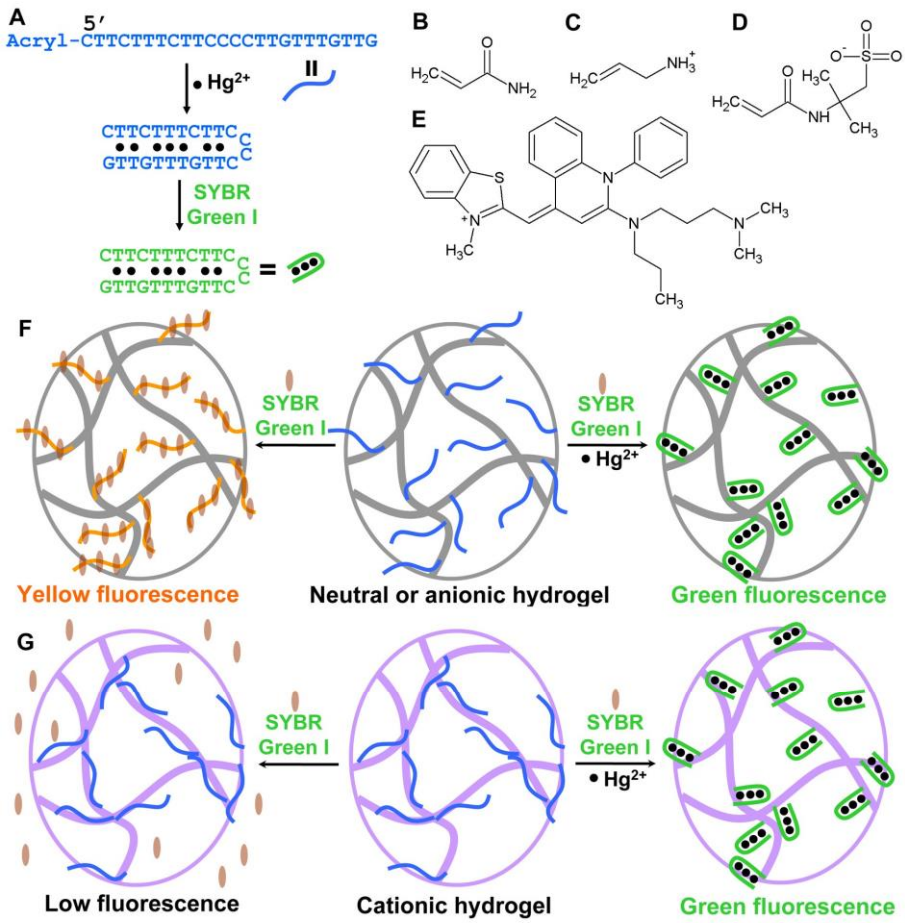

Figure 1. (A) The DNA sequence of the mercury sensing DNA and fluorescence signal generation for Hg^{2+} detection (17). Its 5′-end is modified with an acrydite group for hydrogel attachment. The molecular structures of acrylamide (B), allylamine (C), AMPS (D), and SG (E). Schematic presentation of covalent DNA immobilization within a neutral (polyacrylamide) or negative (containing AMPS) hydrogel (F) or positive hydrogel (containing allylamine) (G). Addition of Hg^{2+} and SG produces a visual fluorescence signal. For the cationic gel, the DNA interacts more with the gel backbone in the absence of Hg^{2+} and the diffusion of SG into the gel is also retarded, giving low background fluorescence.

Effect of monomers on the non-immobilized sensor. Being a soft metal ion, Hg^{2+} can bind to many chemical groups. For example, amine and amide nitrogen are known to bind Hg^{2+} and two of our hydrogel

monomers contain these groups. These monomers may compete with the DNA sensor for Hg^{2+} binding and decrease the sensor sensitivity. To understand the effect of these monomers, the nonimmobilized DNA sensor response was studied. The pH of all three monomers was carefully adjusted to 8.0 with NaOH or HNO_3. The sensor was prepared by mixing 40 nM DNA (Figure 1A, but no acrydite modification) and 240 nM SG in buffer A (8 mM Tris nitrate, pH 8 and 20 mM $NaNO_3$). The sensor response was monitored in the buffer as well as in the presence of 1 and 5% of each monomer.

The Hg^{2+} titration curves are shown in Figure 2B-D, and two observations can be made from this study. First, in the absence of Hg^{2+}, the fluorescence decreased progressively with increasing monomer concentration, suggesting that all the monomers acted as a fluorescence quencher. Acrylamide is known to be a quencher (49), and the quenching effect is expected to reduce after polymerization. Second, while the sensor showed Hg^{2+}-dependent fluorescence increase for all the three monomers at 1%, only the negatively charged AMPS monomer showed an increase at 5% with up to 1 μM Hg^{2+}. This suggests that using our experimental conditions, acrylamide and allylamine bind Hg^{2+} more tightly than AMPS does.

On the other hand, even 1% of the monomers have a molar concentration >40 mM, which is one-million-fold higher than the DNA concentration used in this study. The fact that Hg^{2+} can still be detected in the presence of such high monomer concentration suggests that the DNA binding affinity is more than one-million-fold higher. To prepare hydrogels for visual Hg^{2+} detection, 10 μM DNA was used and the final hydrogel percentages were ~6%. At this concentration, the DNA should be very competitive for Hg^{2+} binding.

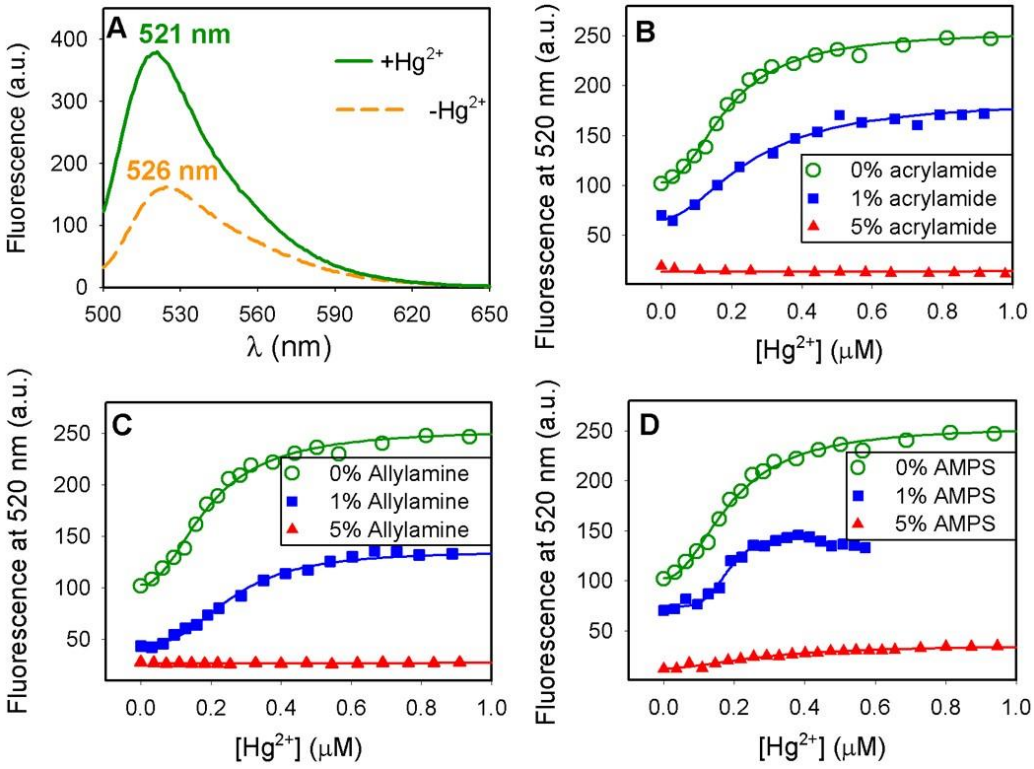

Figure 2. (A) Fluorescence spectra of 6 μM SG and 1 μM DNA in the absence and presence of 4 μM Hg^{2+}. There is an emission wavelength shift upon Hg^{2+} addition, resulting in the fluorescence change from yellow to green. Titration curves of the DNA-based mercury sensor in solution in the presence of varying concentrations of hydrogel monomers of acrylamide (B), allylamine (C) and AMPS (D).

Hydrogel swelling. Unlike neutral acrylamide gels, the charged gels swell more in water because of osmotic pressure and electrostatic repulsion related to the charged polyelectrolyte backbone (19, 50). This is an important factor to consider when designing optical sensors, because the immobilized DNA concentration may decrease significantly due to swelling. We have prepared three gels made of acrylamide and 1:1 (w/w) mixture of acrylamide and the other two charged monomers. If all the gels were prepared with the same initial percentage and volume (e.g. 6% in 75 □L), the negatively AMPS gel swelled the most in water while the polyacrylamide gel maintained its original volume (Figure 3A). The degree of swelling was greatly reduced after soaking the gels in buffer A containing 20 mM $NaNO_3$. To help visualize the gels, 5 μM bromophenol blue dye was added when soaking the gels in water. This dye is

negatively charged and strongly adsorbed by the allylamine gel but repelled by the AMPS gel. This observation suggests that electrostatic interactions can be used to selectively adsorb or repel certain molecules. For example, in the case of cationic SG, the allylamine gel should retard its diffusion into the gel.

The percentage of swelling was quantified by weighing the gels and the results are shown in Figure 3B. The degree of swelling can vary over one order of magnitude depending on the gel composition and buffer conditions. For sensing applications, to ensure a similar final gel percentage and DNA concentration inside the gel for a fair comparison, the starting monomer and DNA concentrations were determined by back calculation.

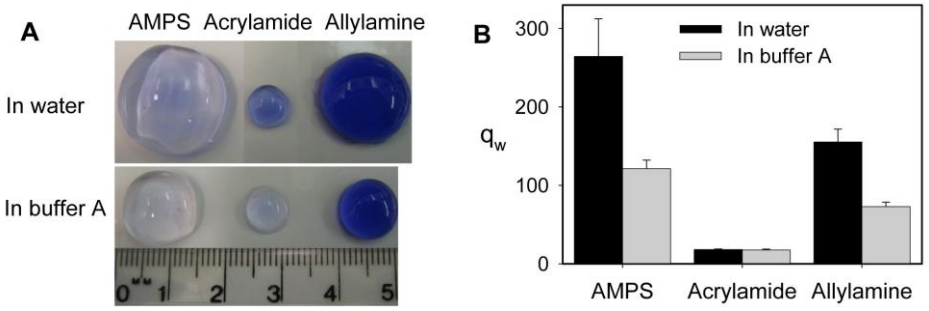

Figure 3. (A) Photographs of differently charged hydrogels swelling in water or in buffer A. 5 μM bromophenol blue was included when soaking in water. (B) Swelling ratio (q_w) of the three kinds of gels in water and in buffer A. The AMPS and allylamine containing gels were made with 1:1 mixture of these two charged monomers and acrylamide.

Effect of hydrogel charge on Hg^{2+} detection. To test the effect of hydrogel charge, three kinds of gels were prepared containing 100% acrylamide, 1:1 allylamine/acrylamide, or AMPS/acrylamide. All the gels were polymerized in the presence of 10 μM acrydite-modified DNA. After removing initiators, free monomers and non-incorporated DNA by soaking in water, the gels were soaked in buffer A containing SG in the presence or absence of 1 μM Hg^{2+}. At designated time points, the gels were observed by exciting them at 365 nm using a hand-held UV lamp. The fluorescence was strong enough to be seen by the eye and was recorded using a digital camera. As shown in Figure 4A and B, both the neutral and negative gels showed a strong yellowish fluorescence in the absence of Hg^{2+} and green fluorescence in the presence of Hg^{2+}. If the fluorescence intensity was compared, the negatively charged gels were the highest followed by the neutral gels, consistent with the cationic nature of the SG dye. The fluorescence intensities were relatively stable after 1 hr for the negative and neutral gels but decayed gradually for the positively charged ones (see Supporting Information). Interestingly, the positively charged gel showed very low background fluorescence in the absence of Hg^{2+} but green fluorescence was observed in the presence of Hg^{2+} (Figure 4C). The reduction of background fluorescence is important for analytical applications, allowing a large room for signal increase. The intensity of the fluorescence, however, was weaker compared to the negative or neutral gels.

DNA is negatively charged and therefore even unfolded ss-DNA can bind to positively charged SG through electrostatic attraction. For negative or neutral gels, the dye can diffuse into the gel quite easily to interact with the DNA. For the positively charged gel, the DNA tends to interact with the gel backbone and the diffusion of the dye into the gel is also disfavored. In particular, the binding affinity between SG and the unfolded DNA is relatively low in the absence of Hg^{2+}. All these interactions help eliminate the background fluorescence. In the presence of Hg^{2+}, the DNA folded into a hairpin, upon which SG can bind with a much higher affinity.

While Hg^{2+} appears to be also positively charged, however, according to thermodynamic calculations, the dominant species at pH 8.0 is the neutral hydroxide $Hg(OH)_2$ (51). Therefore, the effect of gel charge

on the diffusion of mercury species should be relatively small. All the gels were soaked in water before exposed to SG and Hg^{2+}. To highlight the importance of electrostatic interactions, the allylamine containing gel was also soaked in solutions containing 1 and 20 mM Na^{+}. Addition of SG in the absence of Hg^{2+} resulted in a very weak fluorescence for the gel soaked in 1 mM Na^{+} and a relatively strong fluorescence for the one soaked in 20 mM Na^{+} (Figure 4D). Over 90% of the hydrogel mass is water. As a result, the gels are highly porous. The Debye lengths of a charged surface in 1 and 20 mM salt solution are estimated to be 9.6 and 2.2 nm, respectively. Therefore, with 20 mM Na^{+}, the electrostatic effect became too short-ranged to cover the gel pore size, resulting in increased background fluorescence. To confirm that the observed green fluorescence was indeed due to Hg^{2+}-induced DNA folding, another control experiment was performed where the thymine-rich DNA was replaced with a cytidine-rich DNA in the cationic gels (Figure 4E), and no fluorescence was observed even in the presence of Hg^{2+}. This confirms that thymine binding to Hg^{2+} as drawn in Figure 1A was responsible for the hydrogel fluorescence change.

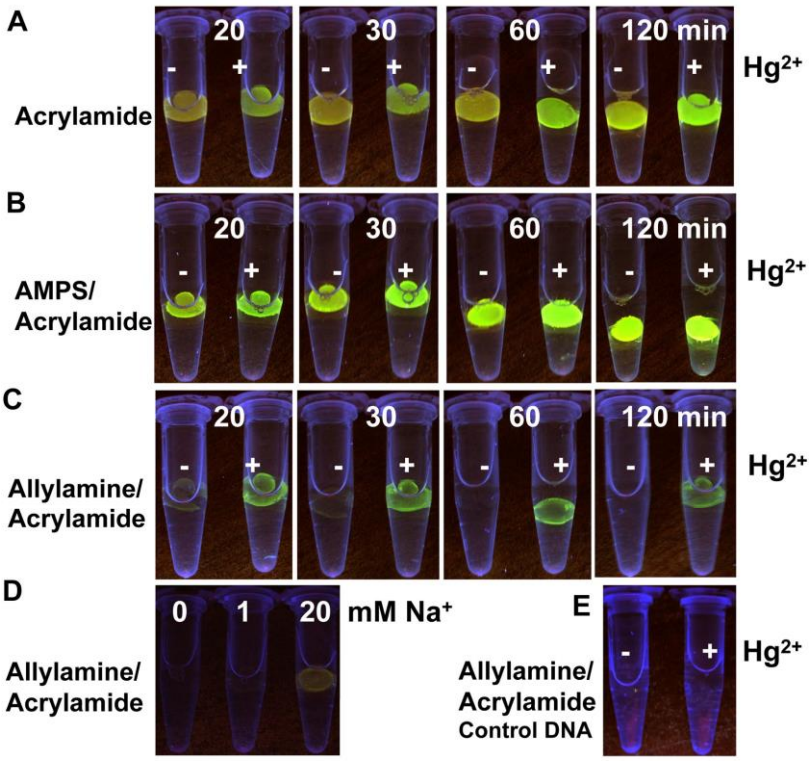

Figure 4. Kinetics of fluorescence change for the three kinds of gels in the presence and absence of 2 μM Hg^{2+}. (A) acrylamide gel; (B) AMPS/acrylamide gel; and (C) allylamine/acrylamide gel. (D) Background fluorescence of the cationic gels soaked in water or in solution containing 1 mM or 20 mM Na^{+} before adding SG. (E) A control experiment with the cytidine-rich DNA functionalized allylamine gels.

Fine tuning the charge effect. In the above experiment, a 1:1 ratio of allylamine and acrylamide was used (i.e. 50% allylamine). While the background fluorescence in the absence of Hg^{2+} was completely eliminated, the signal in the presence of Hg^{2+} was much weaker compared to the other two gel formulations. This suggests that even after DNA binding to Hg^{2+}, the SG and DNA interaction was still adversely affected by the highly positively charged gel matrix. To optimize the allylamine containing gels, the percentage of allylamine relative to acrylamide was systematically varied. As shown in Figure 5, after 30 min, the background fluorescence in the absence of Hg^{2+} decreased progressively with increasing percentage of allylamine. In the presence of Hg^{2+}, the fluorescence changed from a homogenous yellowish

green to green and the green fluorescence appeared to be more intense at the edges. At 60 min, further reduced background fluorescence was observed for the more positively charged gels, although the signal in the presence of Hg^{2+} also decreased. We chose 20% allylamine for subsequent experiments since the background was almost dark and the green fluorescence in the presence of Hg^{2+} was still quite strong.

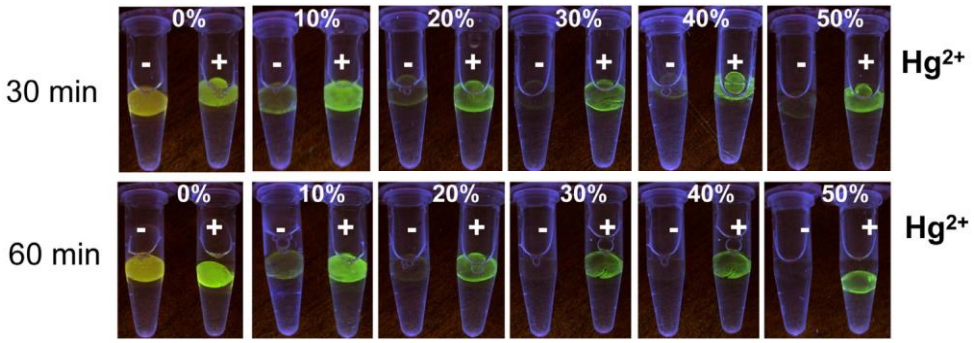

Figure 5. Photographs of hydrogels prepared with varying allylaime/acrylamide ratios in the presence or absence of 2 μM Hg^{2+}. For example, 30% means the starting monomer contained 30% allylamine and 70% acrylamide while the overall gel percentage was ~6%.

Sensor Performance. With the optimized hydrogel formulation, we next tested the sensor sensitivity and selectivity for mercury detection. Hydrogels composed of 20:80 allylamine/acrylamide were prepared and soaked overnight in 50 mL water samples containing varying concentrations of Hg^{2+}. After soaking, the gels were transferred into 1 mL of buffer A to which SG was added at a final concentration of 1.5 μM. The gels were soaked for an additional hour at room temperature and imaged. As can be observed from Figure 6A, as low as 10 nM Hg^{2+} can be easily detected by visual inspection and the background fluorescence in the absence of Hg^{2+} was quite low. If quantified by a gel documentation system (image shown in the lower panel of Figure 6A), ~3-fold fluorescence increase was obtained (Figure 6E, black curve) and the detection limit was determined to be 1.1 nM based on 3σ/slope calculation, where σ is the standard deviation of background fluorescence in the absence of Hg^{2+}. For comparison, the performance

of neutral (Figure 6B) and anionic gels (Figure 6C) under the same condition was also tested. The neutral polyacrylamide gel can visually detect 10 nM Hg^{2+} and a detection limit of 10.2 nM was obtained (Figure 6E, red curve). In terms of intensity change, the neutral gel increased only 55% in the presence of 100 nM Hg^{2+}. The negative charged gel can detect ~20 nM Hg^{2+} visually, and based on the intensity quantification, a detection limit of 56.5 nM was obtained. The improved detection limit for the cationic gel compared to the neutral one comes mainly from the higher slope of the calibration curve; while the worse detection limit for the anionic gel is resulted from the higher background variation. We further tested the performance of the 20% allylamine gel for detecting Hg^{2+} in spiked Lake Ontario water. As shown in Figure 6D, 50 nM Hg^{2+} can be visually detected. The background fluorescence, however, was also quite strong, which was contributed to the relatively high ionic strength of the lake water (52). As mentioned previously, for electrostatic interactions to be effective in porous hydrogels, the solution ionic strength needs to be low. Finally, we tested the selectivity of the cationic gel sensor in the presence of 1 μM various competing metal ions (a total of 13 tested) and all the gels showed low background fluorescence (Figure 6F), suggesting that the high selectivity of the DNA for mercury binding was maintained also in the cationic gel matrix.

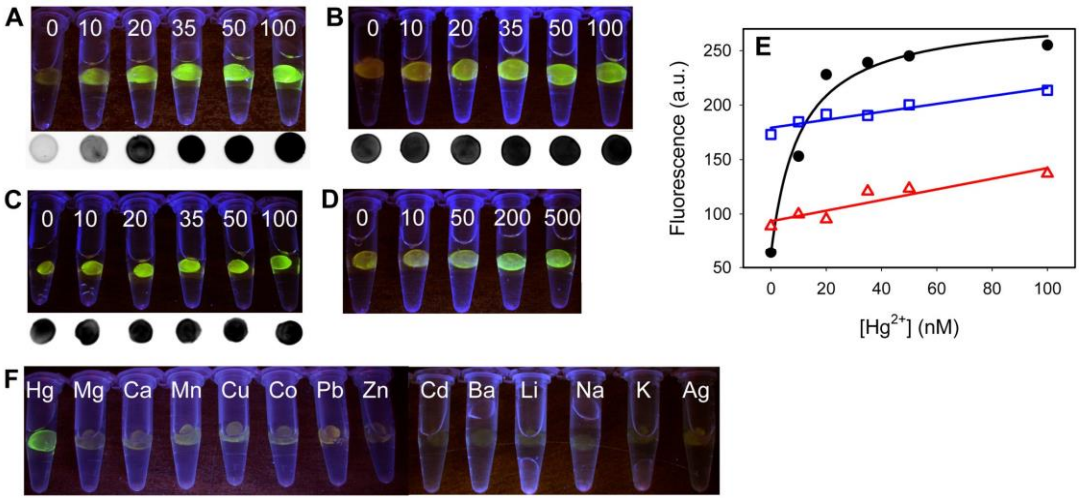

Figure 6. Hydrogel mercury sensor sensitivity obtained using a digital camera (the top panels) and a gel documentation system (the lower panels) for cationic (20% allylamine) (A), neutral (B) and anionic gels (C). (D) Detection of Hg^{2+} in Lake Ontario water using the 20% allylamine gels. The numbers on the top of each sample are Hg^{2+} concentrations in nM. (E) Responses of the sensors quantified using the gel documentation system. Cationic gel: black dots; neutral gel: red triangles; negative gels: blue squares. (F) Sensor selectivity test with 1 μM metal ion each.

CONCLUSIONS. In summary we have prepared and tested DNA-functionalized hydrogels with various gel backbone charges for visual fluorescent mercury detection. Through rational tuning electrostatic interactions, the interaction between the immobilized DNA and SG can be controlled. Importantly, we were able to improve the signal-to-background ratio by six-fold and detection limit by nine-fold through tuning the gel charge. This work indicates that hydrogel is a unique matrix for immobilization of biosensors. Tunable physical properties, high loading capacities and low optical background can be achieved using hydrogels.

ACKNOWLEDGMENT. Funding for this work is from the University of Waterloo and the Discovery Grant from the Natural Sciences and Engineering Research Council of Canada (NSERC).

Supporting Information Available. Kinetics of hydrogel fluorescence intensity change. This material is available free of charge via the Internet at http://www.acs.org.

References:

(1) Nagahara, S.; Matsuda, T. *Polymer Gels and Networks* **1996**, *4*, 111-127.

(2) Lin, D. C.; Yurke, B.; Langrana, N. A. *J. Mater. Res.* **2005**, *20*, 1456-1464.

(3) Murakami, Y.; Maeda, M. *Macromolecules* **2005**, *38*, 1535-1537.

(4) Murakami, Y.; Maeda, M. *Biomacromolecules* **2005**, *6*, 2927-2929.

(5) Um, S. H.; Lee, J. B.; Park, N.; Kwon, S. Y.; Umbach, C. C.; Luo, D. *Nat. Mater.* **2006**, *5*, 797-801.

(6) Liedl, T.; Dietz, H.; Yurke, B.; Simmel, F. *Small* **2007**, *3*, 1688-1693.

(7) Yang, H. H.; Liu, H. P.; Kang, H. Z.; Tan, W. H. *J. Am. Chem. Soc.* **2008**, *130*, 6320-6321.

(8) Lee, Chang K.; Shin, Su R.; Lee, Sun H.; Jeon, J.-H.; So, I.; Kang, Tong M.; Kim, Sun I.; Mun, Ji Y.; Han, S.-S.; Spinks, Geoffrey M. *et al. Angew. Chem., Int. Ed.* **2008**, *47*, 2470-2474.

(9) Cheng, E. J.; Xing, Y. Z.; Chen, P.; Yang, Y.; Sun, Y. W.; Zhou, D. J.; Xu, L. J.; Fan, Q. H.; Liu, D. S. *Angew. Chem. Int. Ed.* **2009**, *48*, 7660-7663.

(10) Tang, H. W.; Duan, X. R.; Feng, X. L.; Liu, L. B.; Wang, S.; Li, Y. L.; Zhu, D. B. *Chem. Comm.* **2009**, 641-643.

(11) Venkatesh, S.; Wower, J.; Byrne, M. E. *Bioconjug. Chem.* **2009**, *20*, 1773-1782.

(12) Topuz, F.; Okay, O. *Biomacromolecules* **2009**, *10*, 2652-2661.

(13) Soontornworajit, B.; Zhou, J.; Shaw, M. T.; Fan, T. H.; Wang, Y. *Chem. Comm.* **2010**, *46*, 1857-1859.

(14) Soontornworajit, B.; Zhou, J.; Wang, Y. *Soft Matter* **2010**, *6*, 4255-4261.

(15) Zhu, Z.; Wu, C. C.; Liu, H. P.; Zou, Y.; Zhang, X. L.; Kang, H. Z.; Yang, C. J.; Tan, W. H. *Angew. Chem. Int. Ed.* **2010**, *49*, 1052-1056.

(16) Baeissa, A.; Dave, N.; Smith, B. D.; Liu, J. *ACS Appl. Mater. Inter.* **2010**, *2*, 3594-3600.

(17) Dave, N.; Huang, P.-J. J.; Chan, M. Y.; Smith, B. D.; Liu, J. *J. Am. Chem. Soc.* **2010**, *132*, 12668–12673.

(18) Kang, H.; Liu, H.; Zhang, X.; Yan, J.; Zhu, Z.; Peng, L.; Yang, H.; Kim, Y.; Tan, W. *Langmuir* **2011**, *27*, 399-408.

(19) Rubinstein, M.; Colby, R. H.; Dobrynin, A. V.; Joanny, J. F. *Macromolecules* **1996**, *29*, 398-406.

(20) Fatin-Rouge, N.; Milon, A.; Buffle, J.; Goulet, R. R.; Tessier, A. *J. Phys. Chem. B* **2003**, *107*, 12126-12137.

(21) Cappuccio, F. E.; Suri, J. T.; Cordes, D. B.; Wessling, R. A.; Singaram, B. *J. Fluoresc.* **2004**, *14*, 521-533.

(22) Shen, Y.; Mackey, G.; Rupcich, N.; Gloster, D.; Chiuman, W.; Li, Y.; Brennan, J. D. *Anal. Chem.* **2007**, *79*, 3494-3503.

(23) Tanaka, Y.; Oda, S.; Yamaguchi, H.; Kondo, Y.; Kojima, C.; Ono, A. *J. Am. Chem. Soc.* **2007**, *129*, 244.

(24) Nolan, E. M.; Lippard, S. J. *Chem. Rev.* **2008**, *108*, 3443-3480.

(25) Ono, A.; Togashi, H. *Angew. Chem., Int. Ed.* **2004**, *43*, 4300-4302.

(26) Liu, J.; Lu, Y. *Angew. Chem., Int. Ed.* **2007**, *46*, 7587-7590.

(27) Wang, Z.; Lee, J. H.; Lu, Y. *Chem. Comm.* **2008**, 6005-6007.

(28) Wang, J.; Liu, B. *Chem. Comm.* **2008**, 4759-4761.

(29) Wang, H.; Wang, Y. X.; Jin, J. Y.; Yang, R. H. *Anal. Chem.* **2008**, *80*, 9021-9028.

(30) Chiang, C. K.; Huang, C. C.; Liu, C. W.; Chang, H. T. *Anal. Chem.* **2008**, *80*, 3716-3721.

(31) Ye, B.-C.; Ying, B.-C. *Angew. Chem., Int. Ed.* **2008**, *47*, 8386-8389.

(32) Lee, J.-S.; Han, M. S.; Mirkin, C. A. *Angew. Chem., Int. Ed.* **2007**, *46*, 4093-4096.

(33) Liu, X. F.; Tang, Y. L.; Wang, L. H.; Zhang, J.; Song, S. P.; Fan, C. H.; Wang, S. *Adv. Mater.* **2007**, *19*, 1471-1474.

(34) Liu, C. W.; Hsieh, Y. T.; Huang, C. C.; Lin, Z. H.; Chang, H. T. *Chem. Comm.* **2008**, 2242-2244.

(35) Xue, X. J.; Wang, F.; Liu, X. G. *J. Am. Chem. Soc.* **2008**, *130*, 3244-3245.

(36) Li, D.; Wieckowska, A.; Willner, I. *Angew. Chem. Int. Ed.* **2008**, *47*, 3927-3931.

(37) He, S. J.; Li, D.; Zhu, C. F.; Song, S. P.; Wang, L. H.; Long, Y. T.; Fan, C. H. *Chem. Comm.* **2008**, 4885-4887.

(38) Lee, J.; Jun, H.; Kim, J. *Adv. Mater.* **2009**, *21*, 3674-3677.

(39) Freeman, R.; Finder, T.; Willner, I. *Angew. Chem., Int. Ed.* **2009**, *48*, 7818-7821.

(40) Li, T.; Li, B. L.; Wang, E. K.; Dong, S. J. *Chem. Comm.* **2009**, 3551-3553.

(41) Lu, N.; Shao, C. Y.; Deng, Z. X. *Analyst* **2009**, *134*, 1822-1825.

(42) Liu, S.-J.; Nie, H.-G.; Jiang, J.-H.; Shen, G.-L.; Yu, R.-Q. *Anal. Chem.* **2009**, *81*, 5724-5730.

(43) Zhu, Z.; Su, Y.; Li, J.; Li, D.; Zhang, J.; Song, S.; Zhao, Y.; Li, G.; Fan, C. *Anal. Chem.* **2009**, *81*, 7660-7666.

(44) Miao, P.; Liu, L.; Li, Y.; Li, G. *Electrochem. Comm.* **2009**, *11*, 1904-1907.

(45) Kong, R.-M.; Zhang, X.-B.; Zhang, L.-L.; Jin, X.-Y.; Huan, S.-Y.; Shen, G.-L.; Yu, R.-Q. *Chem. Comm.* **2009**, 5633-5635.

(46) Harris, H. H.; Pickering, I. J.; George, G. N. *Science* **2003**, *301*, 1203.

(47) Tchounwou, P. B.; Ayensu, W. K.; Ninashvili, N.; Sutton, D. *Environ. Toxicol.* **2003**, *18*, 149-175.

(48) Zipper, H.; Brunner, H.; Bernhagen, J.; Vitzthum, F. *Nucleic Acids Res.* **2004**, *32*, e103.

(49) Strambini, G. B.; Gonnelli, M. *Biochemistry* **2009**, *48*, 7482-7491.

(50) De, S. K.; Aluru, N. R.; Johnson, B.; Crone, W. C.; Beebe, D. J.; Moore, J. *J. Microelectromech. Sys.* **2002**, *11*, 544-555.

(51) Morel, F. M. M.; Kraepiel, A. M. L.; Amyot, M. *Ann. Rev. Ecol. Syst.* **1998**, *29*, 543-566.

(52) Dove, A. *Aquat. Ecosyst. Health.* **2009**, *12*, 281-295.